Title

Aberrant Soluble Epoxide Hydrolase and Oxylipin Levels in a Porcine Arteriovenous Graft Stenosis Model

Journal

Journal of Vascular Research, 51(4)

ISSN

1018-1172

Authors

Terry, Christi M

Carlson, Mary L

He, Yuxia

et al.

Publication Date

2014

DOI

10.1159/000365251

Peer reviewed

HHS Public Access

Author manuscript

J Vasc Res. Author manuscript; available in PMC 2015 September 05.

Published in final edited form as:

J Vasc Res. 2014 ; 51(4): 269–282. doi:10.1159/000365251.

Aberrant soluble epoxide hydrolase and oxylipin levels in a porcine arteriovenous graft stenosis model

Christi M. Terry[1], **Mary L. Carlson**[1], **Yuxia He**[1], **Arzu Ulu**[2], **Christophe Morisseau**[2], **Donald K. Blumenthal**[3], **Bruce D. Hammock**[2], and **Alfred K. Cheung**[4,1]

[1]Division of Nephrology and Hypertension, University of Utah, Salt Lake City, Utah

[2]Department of Entomology and Comprehensive Cancer Center, University of California, Davis, Calif

[3]Department of Pharmacology and Toxicology, University of Utah, Salt Lake City, Utah

[4]Medical Service, Veterans Affairs Salt Lake City Healthcare System, Salt Lake City, Utah, USA

Abstract

Synthetic arteriovenous grafts (AVG) used for hemodialysis frequently fail due to neointimal hyperplasia (NH) development at the vein-graft anastomosis. Inflammation, smooth muscle cell and myofibroblast proliferation and migration, likely play an important role in the pathogenesis of NH. Epoxyeicosatrienoic acids (EETs), which are products of catabolism of arachidonic acid by cytochrome P450 enzymes, possess anti-inflammatory, anti-proliferative, anti-migratory and vasodilatory properties that should reduce NH. The degradation of vasculo-protective EETs is catalyzed by the enzyme soluble epoxide hydrolase (sEH). Thus, sEH up-regulation may contribute to NH development by the enhanced removal of vasculo-protective EETs. In the present study, sEH, cytochrome P450 and EETs were examined after AV graft placement in a porcine model to explore their potential roles in AVG stenosis. Increased sEH protein expression, decreased P450 epoxygenase activity, and dysregulation of five oxylipin mediators were observed in the graft-venous anastomotic tissues compared to control veins. Pharmacological inhibitors of sEH decreased growth factor-induced migration of smooth muscle cells and fibroblasts, although they had no significant effect on proliferation of these cells. These results provide insights on epoxide biology in vascular disorders and rationales for the development of novel pharmacotherapeutic strategies to prevent AVG failure due to NH and stenosis.

Keywords

soluble epoxide hydrolase; P450 epoxygenase; oxylipins; neointimal hyperplasia and arteriovenous-graft stenosis

Dr. Alfred K. Cheung, Division of Nephrology and Hypertension, University of Utah, 85 North Medical Drive East, Salt Lake City, UT 84112 (USA), alfred.cheung@hsc.utah.edu.

Disclosure: There are no competing interests declared for any of these authors.

Introduction

Stenosis with subsequent thrombosis due to underlying neointimal hyperplasia (NH) that forms most often at the vein-graft anastomosis is the major cause of failure of synthetic arteriovenous grafts (AVG) used for chronic hemodialysis.[1, 2] Typically, AVG patency rates are 40% after the first year and decrease to 20% in three years.[3] Strategies to prevent NH formation in AVG are urgently needed.

While many factors contribute to NH development in the AVG, inflammation appears to play a major role as the synthetic graft material is a stimulus to foreign-body inflammatory responses.[4, 5] In addition, the surgical placement of the AVG i) initiates injury to the barrier and vasculo-protective functions of the luminal endothelial cell layer, ii) activates platelets to release inflammatory and pro-proliferative proteins, iii) triggers dedifferentiation of smooth muscle cells to become proliferative and migratory, and iv) upregulates transforming growth factor-β expression that promotes the transition of adventitial fibroblasts into proliferative and secretory myofibroblasts that deposit extracellular matrix.[4, 6-10] The shunting of arterial blood directly into the venous circulation also results in highly disturbed blood flow patterns at the vein-graft anastomosis, which likely induces inflammation and cell proliferation.[11]

Vasoactive arachidonic acid metabolites include the prostanoids produced by cyclooxygenases, the leukotriene and lipoxins generated by the lipoxygenases, and the epoxyeicosatrienoic acids (EETs) which are produced by cytochrome P450 epoxygenases. Oxidative fatty acid metabolites from polyunsaturated fatty acids, such as linoleic acid and eicosapentaenoic acid have been implicated in vascular homeostasis and cytochrome P450 enzymes also produce hydroxylated metabolites, such as 20-hydroxyeicosatetraenoic acid (20-HETE), that possess generally proinflammatory and pro-hypertensive properties. Such oxylipids may also be involved in AVG dysfunction but little is known about their roles in this pathology.

The EETs, produced by cytochrome P450 2C and 2J epoxygenases [12], possess potent biological activities, including the induction of vasodilation, inhibition of inflammation, angiogenesis and cell adhesion, proliferation and migration, as well as inhibition of endothelial cell apoptosis.[13-16] In some cells, EETs inhibit the responses induced by many pro-inflammatory signaling cascades by blocking the activation of lκB kinase, inhibiting the activation and nuclear translocation of the transcriptional regulator nuclear factor κB (NF-κB).[14, 17-19] EETs also can inhibit activation of the inflammation-responsive c-Jun-N-terminal kinase (JNK).[20, 21] EETs attenuate the expression of some cellular adhesion molecules and decrease the aggregation of platelets and polymorphonuclear cells.[22-25] Another beneficial vascular action of EETs is the promotion of endothelial cell proliferation by activation of p38 mitogen-activated protein kinase (MAPK) and the pro-survival phosphotidylinositol 3-kinase/Akt pathways.[26, 27] Thus, EETs play essential roles in maintaining vascular structure and functions.

The bioavailability of EETs is primarily regulated by soluble epoxide hydrolase (sEH).[28] The sEH enzyme is widely distributed in mammalian tissues. It is responsible for the

catabolism of the regioisomeric 5,6-, 8,9-, 11,12-, and 14,15-EET lipid mediators into dihydroxyeicosatrienoic acids (DHETs) that are biologically less active than EETs.[29] The 11,12- and 14,15- isomers are the more prevalent regioisomers in the vasculature and the 14,15- isomer is the preferred substrate for sEH.[13, 30] The sEH enzyme plays a role in vascular remodeling in injury-induced vascular stenosis. For example, pharmacological inhibition of sEH or sEH gene knockout decreased neointimal/medial ratios in a carotid ligation model and in a femoral cuff injury model in hyperlipidemic mice.[31, 32] Pharmacological inhibitors of sEH have been reported to attenuate end organ damage as well as endothelial dysfunction and inflammation in animal models of cardiovascular diseases, such as hypertension, ischemia, and hypertrophy.[33-38] Recently, inverse correlations between plasma EET/DHET ratios and both plasma monocyte chemotactic protein-1 and cellular adhesion molecule levels were observed in patients with coronary artery disease.[39] Inasmuch as a lower EET/DHET ratio is a reflection of elevated sEH activity, this observation suggests that elevated sEH activity participates in the pathogenesis of vascular diseases in humans.

Very recently, an inhibitor of sEH was shown to attenuate cytokine release from human monocyte/macrophages.[40] These intriguing and promising data support the further investigation of oxylipids and sEH in AVG dysfunction.

We hypothesized sEH is over-expressed in the juxta-anastomotic region of the AVG with subsequent reduction in tissue EET levels and their associated vasculo-protective effects. The present study determined in the vascular tissues around the vein-graft anastomosis of the AVG in a porcine model, i) the activities of P450 epoxygenase that catalyzes EET production; ii) the expression and activities of sEH that catabolizes EETs; iii) the cell types and location within the vascular wall in which sEH is expressed; and iv) the tissue oxylipin profile. These studies should provide insights into the potential pathogenic role of epoxyfatty acid dysregulation in NH development in AVG and possibly other vascular disorders, and whether there is a rationale for targeting sEH to prevent AVG failure.

Materials and Methods

Animal model

All animal experiments were performed in accordance with the guidelines established by the *Guidelines for the Care and Use of Laboratory Animals* (NIH Publication No. 85-23, revised 1996). The protocol was approved by the Institutional Animal Care and Use Committees at the University of Utah and Veterans Affairs Salt Lake Healthcare System.

A porcine AVG model was used in which NH develops at the vein-graft anastomosis consistently around 4 weeks after AVG placement.[41, 42] This location of NH is similar to that observed commonly in patients.[43] Yorkshire cross-domestic swine, aged three months and weighing approximately 30 kg, underwent surgical placement of unilateral AVG according to our previously published procedure.[44] Post-operatively, graft patency was monitored weekly using Doppler ultrasound (SonoSite, Bothell, WA) and a L38/10-5 MHz transducer (TITAN, SonoSite).

Surgical Procedures

For the surgical implantation of the AV graft, oral aspirin EC (81 mg/day; Phamaceutical Formulations, Edison, NJ) and clopidogrel (225 mg/day; Bristol-Myers Squibb, New York, NY) were administered peri-operatively. Enrofloxacin (5 mg/kg; Bayer, Pittsburgh, PA) was administered intra-muscularly on the day of surgery and daily for the first three days after surgery. The animals underwent tracheal intubation after anesthetization with an intramuscular injection of xylazine (4 mg/kg), tiletamine/zolazepam (Telazol®) (4 mg/kg) (Fort Dodge Animal Health, Fort Dodge, IA), and ketamine (4 mg/kg) (Hospira Inc., Lake Forrest, IL). Anesthesia was maintained with inhalation of 1-3% isoflurane. Intravenous sodium heparin (100 units/kg; Baxter, Deerfield, IL) was administered intra-operatively. A 7-cm long, 6-mm internal diameter, externally spiral-reinforced expanded polytetrafluoroethylene (ePTFE) graft (Bard Peripheral Vascular Inc., Tempe, AZ) was placed between the common carotid artery and the ipsilateral external jugular vein.

Graft and tissue explantation and processing

Juxta-anastomotic venous tissues were obtained at various time points (1 day, 3 days, 1 week, 3 weeks, or 4 weeks) as previously described.[44] For immunohistofluorescence, tissue sections were fixed in formalin. For all other assays, the explanted vessels were flash-frozen in liquid nitrogen. Tissues from pigs were used for histology (n=13), immunoblotting (n=5), sEH and P450 epoxygenase activity assays and oxylipin profiling (n=4).

Immunoblotting analysis of tissue and cell lysates

Frozen juxta-anastomotic venous segments explanted 1 week (n=1) or 3 weeks (n=2) after graft placement were lysed in buffer containing Complete Mini protease inhibitor cocktail (Roche Diagnostic, Mannheim, Germany) and protein concentrations determined by the bicinchoninic acid (BCA) assay (Pierce, Rockford, IL). Twenty-five μg of the vessel lysates were separated on 4-12% NuPAGE® Bis-Tris polyacrylamide gels and transferred to nitrocellulose membrane (Invitrogen, Carlsbad, CA). The membranes were incubated in 5% dry-milk blocking buffer then overnight at 4°C with a 1:2500 dilution of polyclonal rabbit anti-porcine-sEH antibody [45] and a 1:10,000 dilution of monoclonal rabbit-anti-human GAPDH (Cell Signaling, Danvers, MA). Ten μg of lysate from porcine or human cultured SMC or murine liver were subjected to SDS-PAGE on 10% gels and transferred to nitrocellulose membranes that were incubated with a 1:200 dilution of rabbit anti-human CYP2J2 (Santa Cruz Biotechnology, Santa Cruz, CA), or a 1:1000 dilution of rabbit anti-human sEH (Santa Cruz Biotech.). For the peptide blocking experiment, anti-sEH antibody was preincubated with sEH-specific blocking peptide (Santa Cruz Biotech.) prior to immunoblotting. The membranes were washed in Tris-buffered saline/Tween solution (TBST) and incubated with a secondary goat anti-rabbit IgG conjugated to horseradish peroxidase (Santa Cruz Biotechnology). Supersignal® West Dura Extended Duration Substrate kit (Thermo Scientific, Rockford, IL) was used for chemiluminescent antibody detection on autoradiography film. Densitometry of each band of interest (sEH or GAPDH) was quantified using the Kodak Molecular Imaging Software v 4.5.1 (Molecular Imaging Systems, Carestream Health, Inc., Rochester, NY).

Immunohistofluorescence analysis

Formalin-fixed and paraffin-embedded tissues were deparaffinized and rehydrated using non-xylene Aqua DePar and Hot Rinse ancillary reagents (Biocare Medical, LLC, Concord, CA). Antigen retrieval was performed using 10 mM sodium citrate in an EZ-Retriever System (BioGenex Laboratories Inc., San Ramon, CA). Nonspecific binding was blocked with 2% goat serum and the tissue was incubated overnight at 4°C with a rabbit anti-porcine sEH antibody (1:200) [45] and an antibody directed against a murine monoclonal anti-α-smooth muscle actin conjugated to phycoerythrin (α-SMA-PE, R & D Systems, Minneapolis, MN) or a murine monoclonal anti-smooth muscle myosin heavy chain (SMMHC, Chemicon International Inc., Temecula, CA) at dilutions of 1:100 and 1:150 respectively. Following an overnight incubation and serial washes in TBST, the tissue sections were incubated for 1 hr with an anti-rabbit IgG secondary antibody (Alexa 488 at 1:200 dilution, Invitrogen, Carlsbad, CA) for the detection of sEH, and murine biotin-strepavidin 546 (at 1:200 dilution, Invitrogen) for the detection of SMMHC. After further washing with TBST, a nuclear stain (Dapi-Fluoromount-G, Southern Biotech, Birmingham, AL) was added.

The slides were analyzed using confocal microscopy (BX61, Olympus America Inc., Center Valley, PA) at 200x magnification and excitation wavelengths appropriate for the fluorophores used (405 nm, 488 nm or 543 nm). Photomultipler settings were determined using secondary antibodies alone as negative controls. Ten 1.5-μm slices were generated using the Fluoview FV1000 software (Olympus, Center Valley, PA). The expression of the protein was semi-quantified by determining the pixel intensity in z-stacked images imported into Image J (NIH). The number of DAPI-stained nuclei for each Z-stacked image was also determined and used to calculate the amount of sEH expressed per cell. The sEH expression per cell from two replicate histology sections was averaged for the tissue sample from each animal.

P450 Epoxygenase and sEH activities

Explanted venous tissues were flash frozen at either three weeks (n=3) or six weeks (n=1) after graft placement for metabolomic analysis. For the analysis of P450 epoxygenase activity, samples were thawed and maintained in sodium phosphate buffer with 5 mM EDTA, 1 mM PMSF, 1 mM DTT at 4°C.[46] After homogenization and centrifugation at 10,000 × g for 10 min at 4°C, the supernatant was subjected to protein assay and activity measurements. For epoxygenase activity assessment, arachidonic acid (100 μM) was added to diluted sample extracts and incubated at 37°C. After 5 min, 5 μL of NADPH-generating-system solution (100 mM glucose-6-phosphate, 6 mM $NADP^+$, 6 U/ml glucose-6-phosphate dehydrogenase in 0.1 M phosphate buffer, pH 7.4) was added and incubated for 30 min. Ethanol was then added to the reaction with internal EET standards, vortexed, and centrifuged at 2500 × g at 4°C for 4 min. The supernatants were then assayed by LC/MS/MS for the various EET moieties.

For sEH activities, harvested cells were suspended in 1 ml of chilled sodium phosphate buffer (0.1 M, pH 7.4) containing 1 mM of EDTA, PMSF and DTT. The cells were disrupted using a Polytron homogenizer (9,000 rpm for 30 s). The homogenate was used as

enzyme extract. Protein concentration was quantified using the Pierce BCA assay (Pierce, Rockford, IL), using Fraction V bovine serum albumin (BSA) as the calibrating standard. Epoxide hydrolase activity was measured using racemic [^{3}H]-*trans*-1,3-diphenylpropene oxide (tDPPO) as substrate (Borhan *et al.*, 1995). Briefly, 1 μL of a 5 mM solution of [^{3}H]-tDPPO in DMF was added to 100 μl of enzyme preparation in sodium phosphate buffer (0.1 M, pH 7.4) containing 0.1 mg/ml of BSA ([S]final = 50 μM). The enzyme was incubated at 30°C for 30 min, and the reaction quenched by addition of 60 μl of methanol and 200 μl of isooctane, which extracts the remaining epoxide from the aqueous phase. Extractions with 1-hexanol were performed in parallel to assess the possible presence of gluthation transferase activity which could also transform the substrate. The activity was followed by measuring the quantity of radioactive diol formed in the aqueous phase using a scintillation counter (Tri-Carb 2810 TR, Perkin-Elmer, Shelton, CT).[47] Assays were performed in triplicate.

Tissue oxylipin analysis

Fifty milligrams of porcine anastomotic vein tissues from three animals, obtained at three weeks after graft placement, or the contralateral unoperated vein tissues, were weighed and kept at -20°C for 30 min with 10 μL of an anti-oxidant solution (0.2 mg/ml butyl hydroxytoluene (BHT) and EDTA), 10 μL internal standard and 400 μL ice-cold methanol containing 0.1% acetic acid and 0.1% BHT. The tissues were homogenized using metal beads in a tissue grinder (Glen Mills Inc, NJ) at 30 Hz for 10 min. Resulting homogenates were stored at -20°C overnight and centrifuged at 10,000 rpm at 4°C for 10 min. The supernatant was collected and the remaining pellets were washed with 100 μL of ice-cold methanol containing 0.1% acetic acid and 0.1% BHT. All collected supernatants were diluted with 2 mL distilled water and oxylipins were extracted using solid-phase extraction. After the samples were passed through a C18 cartridge (Waters Oasis HLB C18 cartridge), the bound oxylipins were eluted using ethyl acetate and samples were evaporated to dryness with a vacuum centrifuge. The samples were then re-dissolved with 50 μL additional standard solution (instrumental standard) in methanol and measured using mass spectrometry.[48]

Cell proliferation and migration studies

The compounds *trans*-4-(4-{1-adamantyl-ureido}-cyclohexyloxy)-benzoic acid (t-AUCB) and 1-(1-Adamantyl)-3-(dodecanoic acid)urea (AUDA) are selective inhibitors of human sEH, with 50% inhibition (IC_{50}) of 1.3 ± 0.1 nmol/L and 3.0 ± 0.5 nmol/L, observed in biochemical assays respectively.[49, 50] Smooth muscle cells (SMC) and adventitial fibroblasts were isolated from normal porcine jugular vein using published techniques.[51] Human aortic SMC and fibroblasts (Cambrex Bio Science, Chicago, IL) as well as porcine venous SMC and fibroblasts (passages 5-8) were seeded into 96-well tissue culture plates at subconfluence and made quiescent by incubation in media with no serum for 48 hr. The cells were pretreated with either dimethylsulfoxide (DMSO) alone or a sEH inhibitor (AUDA or *t*-AUCB) at 0.1- 10 μM in the absence or presence of EETs (11,12- or 14,15-EET, Cayman Chemical, Ann Arbor, MI) for 1 hr. Cell proliferation was stimulated with either PDGF-AB (50 ng/mL) (R&D Systems, Minneapolis, MN) or 10% FBS for 48 hr and assessed with a colorimetric assay following the manufacturer's protocol (CellTiter 96 AQueous One, Promega, Madison, WI). The wounding assay was used for assessing cell

migration and was performed by seeding the cells to subconfluence onto four-chamber slides (Lab-TekII, Nunc, Rochester, NY). Quiescent cells were then wounded by dragging a pipet-tip across the middle of each chamber. The chambers were washed and medium containing PDGF-AB (50 ng/mL) was added to each chamber with or without imatinib (10 μM) (Gleevec, Novartis Pharmaceuticals Corp., East Hanover, NJ) or AUDA (10 μM) and incubated for 24 hr. The cells were then fixed in methanol and stained with the Diff-Quick® stain set (Dade Behring, Inc., Newark, DE).

For the migration studies, human aortic SMC or human adventitial fibroblasts were serum-starved for 24 hr and pretreated with either DMSO or one of the sEH inhibitors, t-AUCB or AUDA, at 1 μM or 5 μM for 1 hr. After pretreatment, the cells were seeded onto the upper well of a migration chamber insert (InnoCyte™ 96-well, Calbiochem, La Jolla, CA) containing a porous 8-μm membrane separating the upper and lower chambers. Chemotaxis was stimulated by the addition of PDGF-AB (25 ng/ml) to minimal culture medium in the lower chamber of the 96-well migration plate. Cells were incubated at 37°C in a humidified chamber with 5% CO_2 for 15 hr and then processed according to the manufacturer's instructions for cell detachment and Calcein-AM labeling. Fluorescence quantification of the migrated cells was determined by a fluorescent plate reader with excitation and emission wavelengths of 485 nm and 520 nm respectively.

Statistical analysis

Values of sEH expression by immunohistofluorescence staining of tissues obtained from juxta-anastomotic venous tissue sections were compared to those obtained from the control external jugular veins using unpaired Student's t-tests. Separate analyses were performed to compare venous anastomotic tissues obtained from the early postoperative period (within one week; n=5) to controls and to compare venous anastomotic tissues obtained at late time points (3–4 weeks; n=4) to controls. A p value < 0.05 was considered to be statistically significant.

An analysis of variance was used to compare the log-transformed tissue levels of 8,9-EETs, 11,12-EETs and 14,15-EETs between the venous anastomotic tissues and control veins. The analysis of variance model included separate factors for the various EETs and for the comparison between the venous anastomosis and control vein, with the individual animal treated as a blocking factor. This analysis was used to perform a pooled comparison of the log-transformed tissue levels between the venous anastomosis and control vein across the three substrates (EETs), and to evaluate if the difference of log-transformed tissue levels between the venous anastomosis and control vein differed among the three substrates.

In exploratory analyses, separate paired t-tests were performed to compare log-transformed tissue levels for 32 oxylipins between venous anastomosis and control vein, with results expressed as the ratio of geometric means with 95% confidence intervals. These exploratory analyses were performed on a comparison-wise basis, without adjustment for multiple comparisons. Additionally, an unpaired student t-test was used to evaluate differences in fluorescent intensities between cells migrating in the presence or absence of sEH inhibitors in the migration assay. A p value <0.05 was considered significant.

Results

Immunoblotting of sEH in the tissues of the vein-graft anastomosis

Because stenotic lesions occur most frequently at the vein-graft anastomosis, lysates were prepared from the anastomotic venous tissues (Fig. 1A) from pigs at one or three weeks after surgical graft placement. Lysates were also obtained from external jugular veins from un-operated normal pigs that served as controls. Levels of sEH protein were determined by immunoblotting. A protein band with apparent molecular weight of 62 kD was detected with the anti-porcine sEH antibody (Fig. 1B). Densitometric quantification of these bands showed a 2-fold increase in sEH protein in the vein-graft anastomosis tissue, compared to levels observed in control veins (Fig. 1B).

Immunohistofluorescence of sEH in the tissues of the vein-graft anastomosis

Immunohistofluorescence of anastomotic venous tissues was used to confirm the immunoblot finding of elevated sEH expression and to identify the location of the sEH within the vascular wall. The expression of sEH increased in the anastomotic venous tissues early (one week) after graft placement, compared to control jugular veins (Fig. 2A). The increased sEH staining was most prominent in the adventitial layer at one week, persisting to three (Fig. 2A and 2B) and four weeks, the longest time point examined (data not shown). At three weeks, increased sEH expression was also apparent in the medial layer (Fig. 2A). Expression of sEH was high in the luminal endothelium of control vein but was decreased in a sporadic fashion in the endothelium at later time points (Fig. 2A). The expression of sEH in the entire tissue section was quantified by measurement of pixel intensity of the sEH staining. Even after normalization against the cell number, the increased expression of sEH was apparent within one week (early) and remained increased at 3-4 weeks (late), compared to control veins (Fig. 2B).

Immunohistochemical staining with anti-von Willebrand factor antibody revealed some loss of endothelial cells at the anastomotic venous tissues one week after AVG placement (data not shown), likely due to surgical trauma. Co-staining of sEH and von Willebrand factor was unsuccessful despite repeated attempts. Thus, it could not be determined if the diminished sEH immunostaining in the luminal cells was a result of decreased sEH expression or the loss of endothelial cells. Numerous small vessels that stained positive for sEH were observed in the adventitia at the later time points.

Types of cells expressing sEH in the tissues of the vein-graft anastomosis

Both differentiated quiescent SMC of normal venous vessels, and dedifferentiated synthetic SMC express smooth muscle a-actin (SMA). Fibroblasts that have dedifferentiated to the migratory and proliferative myofibroblast phenotype acquire the expression of SMA. In contrast to SMA, smooth muscle myosin heavy chain (SMMHC) is expressed exclusively by differentiated quiescent SMC only. Thus, an *increase* in SMA expression and a *decrease* in SMMHC expression suggest the dedifferentiation of quiescent contractile SMC to the proliferative, synthetic SMC phenotype and/or the presence of myofibroblasts. Such cells are associated with NH development. Co-immunostaining experiments were performed to examine the co-localization of sEH expression with SMA and SMMHC expression in the

vessel wall. The co-expression of sEH and SMA in the control veins was limited in nature and confined to the medial layer (Fig. 3A, **first row**). In contrast, in the anastomotic venous tissues collected at one week, the co-immunostaining for sEH and SMA was much stronger, *increased* over time, and occurred in the adventitia (Fig. 3A, **second and third rows**). In contrast, co-immunostaining for sEH and the marker for contractile differentiated SMC (SMMHC) in the medial layer in AVG *decreased* over time compared to control vein (Fig. 3B). These data suggest that an increase in sEH expression in the tissue at the vein-graft anastomosis is associated with dedifferentiation of SMC to a more synthetic, proliferative and migratory phenotype.

In addition to the medial layer, co-staining for sEH and SMA was strong in the NH at one week and three weeks (Fig. 3A) but co-staining for sEH and SMMHC was very low in these regions (Fig. 3B), suggesting the sEH-expressing cells in the NH were dedifferentiated SMC or myofibroblasts. Numerous neovessels were observed at 3-4 weeks after graft placement (Fig. 3A and 3B).

P450 Epoxygenase and sEH activities in tissues of the vein-graft anastomosis

The levels of 8,9-EET, 11,12-EET, and 14,15-EET, products of tissue P450 epoxygenase activity, were evaluated in tissue obtained at 3 weeks from the vein-graft anastomosis, and from control veins. The mean P450 epoxygenase activity to produce all three EETs combined was 3.1 pmol/min/mg in the anastomotic tissues of three animals and 6.4 pmol/min/mg for the three control veins (Fig. 4). ANOVA analysis after log transformation of epoxygenase activity data showed that epoxygenase activities were significantly lower ($p< 0.001$) in anastomotic tissues than those in the control veins for those EET moieties; the ratio of geometric means of anastomosis to control was 0.54 (95% confidence interval 0.42-0.71). No difference was observed for the epoxygenase activities generating 5,6-EET (data not shown), an epoxide that is less prevalent and less stable than the three aforementioned EETs. Activity of sEH was also measured in these tissues, but the results were highly variable amongst animals and there was no significant difference in mean sEH activity between the venous anastomotic tissues at the three-week time point, and control veins (101.0 + 54.9 pmol/min/mg vs. 84.7 ± 70.2 pmol/min/mg, respectively). Venous anastomosis tissue from one pig collected six weeks after graft placement, however, displayed increased sEH activity (77.3 pmol/min/mg) compared to the unoperated femoral vein (19.5 pmol/min/mg).

Oxylipin levels in tissues of the vein-graft anastomosis

A profiling of 38 oxylipin levels was performed on the vein-graft anastomotic tissue of three animals three weeks after AVG placement and compared to levels in unoperated control veins. Five of the assayed oxylipins were below the limit of detection. Levels of 28 oxylipins were similar between control veins and anastomotic tissues (Table 1). However, vein anastomotic tissues had significantly decreased levels of three oxylipins: 9-, and 13-hydroxyoctadecadienoic acid (9-HODE, 13-HODE), and 12,13-dihydroxyoctadecenoic acid (12,13-DiHOME) by 3.0-fold, 2.1-fold and 1.5-fold respectively ($p < 0.05$ by ANOVA) (Fig. 5). In contrast, prostaglandin D_2 (PGD_2) and 12-hydroxyeicosatetraenoic acid (12-

HETE), were found to be significantly increased by 2.0 and 5.7-fold respectively in the anastomotic tissues, compared to control veins ($p < 0.05$) (Fig. 5).

Effect of epoxyeicosatrienoic acid and sEH inhibitor on cell proliferation and migration

Immunoblotting of lysates from cultured porcine or human SMC detected sEH protein (Fig. 6A, **left blot**). The P450 epoxygenase isoform CYP2J2 metabolizes arachidonic acid to EETs, and its expression was detected in cultured SMC (Fig. 6A, **right blot**). However, neither 11,12-EETs nor the combination of EETs and the sEH inhibitor, AUDA, significantly affected proliferation of SMC (Fig. 6B). Other EETs and different concentrations of AUDA were tested but also showed no significant effect (data not shown). Fig. 6C shows that AUDA alone had no significant affect on adventitial fibroblast proliferation. Exposure to EETs or AUDA plus EETs also did not significantly affect fibroblast proliferation (data not shown). Exposure to 14,15-EET and/or another pharmacological sEH inhibitor also did not attenuate proliferation (data not shown).

The effects of EETs and/or sEH inhibitor on SMC chemotaxis was determined by both a wounding assay and a Boyden chamber-type assay. Fig. 7 shows that AUDA attenuated PDGF-induced human aortic SMC migration across a wound area similar to that observed with imatinib, a PDGF receptor kinase inhibitor. Similarly, two different inhibitors of sEH, *t*-AUCB and AUDA, attenuated PDGF-induced SMC migration and adventitial fibroblast migration through a porous filter (Fig. 8).

Discussion

Cytochrome P450 epoxygenases metabolize arachidonic acid to EETs which have anti-inflammatory, vasodilatory and other vasculoprotective properties, while sEH rapidly catabolizes the EETs. Other studies have reported the efficacy of sEH inhibitors in attenuating atherosclerosis, abdominal aortic aneurysm formation and hypertension-induced NH in various animal models.[31-38] This study addressed the potential role of altered epoxygenase and sEH pathways in the pathogenesis of NH associated with AVG in a large animal model.

The expression of sEH was low in the media and adventitia of control unoperated vein but increased early and remained elevated for several weeks in the tissue of the vein-graft anastomosis region after AVG placement. Increased sEH expression was predominant in the medial SMCs and cells in the adventitia, concomitant with the appearance of synthetic dedifferentiated SMC and/or myofibroblasts, as determined by increased expression of SMA, a marker of dedifferentiation. Dedifferentiation of SMC and fibroblasts to a more synthetic phenotype occurs with vascular trauma and results in greater proliferative and migratory capacity as well as increased synthesis of collagen and other extracellular matrix proteins.[52-54] We previously reported that adventitial cells become highly proliferative soon after AV graft placement in the porcine model and that these cells, as well as the medial SMC, likely contribute to NH by migrating to the neointima.[55] The early onset and prolonged increase in sEH protein expression in SMC and adventitial cells is consistent with the notion that elevated sEH expression is important in the development of NH in AVGs.

In the current study, exogenous EETs and/or pharmacological inhibitors of sEH had little effect on SMC or fibroblast proliferation. In other studies, EETs alone also failed to influence SMC proliferation.[16, 56] However, it was previously reported that an sEH inhibitor, different than that used in the current study, attenuated SMC proliferation.[57] The inhibitory effect was later shown to be unrelated to sEH inhibition.[58] Ng et al, did report that AUDA and EETs inhibited PDGF-BB-induced proliferation of aortic SMC.[59] These conflicting results could be due to differences in the source (aortic vs. venous or pulmonary) of the SMC, and/or isoform of the growth factor (PDGF-BB vs. PDGF-AB), or concentration of PDGF employed, and/or timing of the drug exposure, in the different studies.

Although neither SMC or fibroblast proliferation was inhibited in the current study, SMC migration was significantly attenuated by sEH inhibitors, similar to that reported by Sun [16]. Previous work by our group has also shown that macrophage accumulation and cytokine expression are pronounced features of AVG stenosis and that a pharmacological inhibitor of sEH caused a significant decrease in release of monocyte-chemotactic protein-1 and TNF from lipopolysaccharide-stimulated human monocytes *in vitro*.[40] The data presented herein, together with previous works, suggest that sEH inhibition could be useful for the prevention of AVG stenosis by both targeting inflammation as well as cell migration.

Decreased activity of the P450 epoxygenases that produce EETs was observed in the vein-graft anastomosis tissue (Fig. 4), suggesting a decreased production of EETs in the vein-graft tissue compared to control vein tissue. However, no significant difference in 8,9-, 11,12- or 14,15-EET levels (Table 1) was observed in those same lysates even though the western blotting and immunohistochemical studies showed increased sEH protein levels in the vein-graft tissue. Graft placement triggers drastic changes in blood flow rate and patterns in the vein, and consequently may cause changes in gene expression in the ungrafted contralateral vessels. It is also possible that there were concomitant compensatory decreases in other EET breakdown pathways in the vein-graft tissue. There were significant decreases in 12,13-DiHOME (an isoleukotoxin diol product of the P450 epoxygenase pathway), 9-HODE and 13-HODE (produced during the oxidation of low-density lipoprotein LDL). The 12,13-DiHOME, 9-HODE and 13-HODE are endogenous activating ligands for peroxisome proliferator activated receptor gamma (PPAR-γ).[60-62] Activation of PPAR-γ decreases vascular SMC proliferation and migration [63, 64] and inhibits the activation of macrophages.[65, 66] Thus decreases in these oxylipin PPAR-γ agonists after AVG placement may contribute to prolonged inflammation and potentiate NH formation.

Two pro-inflammatory eicosanoid mediators, PGD_2 and 12-HETE, were found to be significantly increased at the vein-graft anastomosis. PGD_2 is produced by prostaglandin synthase D_2 and has been shown by *in vitro* studies to be a SMC mitogen released by human umbilical venous endothelial cells following hypoxia.[67] 12-HETE is produced by 12-lipoxygenase activity and has been implicated in angiogenesis, neutrophil aggregation and vasoconstriction.[68-72] Of note, neovessel formation likely supports NH development by providing nutrients to the growing tissues and allowing access for inflammatory cells. Thus the elevated 12-HETE observed in the vein-graft tissue may participate in NH development via promoting neovessel formation.

The various biological activities of the several fatty acid mediators that were found to be dysregulated in the present study are consistent with a role for oxylipins in the pathogenesis of NH in the AVG. Regulation of inflammation and NH in the AVG appears to be complex, as a result of changes in multiple lipid mediators, cytokines, chemokines and other factors. These proposed lipid metabolic pathways are illustrated in Figure 9. Since both the propagation and resolution of inflammation are critical pathophysiological and physiological processes, therapeutic alteration of these processes can have complex outcomes. Nonetheless, targeting sEH and other related key enzymes may be an effective therapeutic strategy to prevent NH in the AVG.

We acknowledge the following limitations to the present work. The porcine model used for this study develops inflammation, neointimal hyperplasia and graft stenosis similar to that seen in humans. However the animals had intact kidney function and it is possible impaired kidney function would accelerate such processes and/or alter sEH expression. This work used a costly and labor-intensive large animal model since arteriovenous grafts cannot reasonably be placed in small animals. The advantage is that data from this model are likely more translatable to patients since the hemodynamics and foreign-body responses are similar to those in humans. Results from the immunoblotting and IHC experiments are consistent with each other and indicate elevated sEH protein in the vein-graft tissue. These results were also supported by elevated sEH activity in one animal analyzed at 6 weeks after graft placement. However, there is a risk of false discovery and caution should be used in interpreting the oxylipin levels and enzyme activity data because of the small number of animals used in the sEH activity experiments. The anti-platelet drugs clopidogrel and aspirin were administered to all animals before and after graft placement surgery. Aspirin is commonly used in chronic hemodialysis patients. It inhibits the cyclooxygenases in the arachidonic acid pathway and may inhibit the production of EETs by competing for the arachidonate substrate. Clopidogrel has no known effects on arachidonate metabolism.

Acknowledgments

Grants: The authors thank Huan Li and Ilya Zhuplatov for performing animal surgeries. This study was supported by the Veterans Affairs Merit Review Program (AKC). Partial support was provided by National Institute of Environmental Health Sciences (NIEHS) (BDH). The statistics analysis was performed by the University of Utah Study Design and Biostatistics Center under the guidance of Tom Greene, with funding in part from the Public Health Services research grant numbers UL1-RR025764 and C06-RR11234 from the National Center for Research Resources. BDH is a George and Judy Marcus Fellow of the American Asthma Foundation.

References

1. Feldman HI, Kobrin S, Wasserstein A. Hemodialysis vascular access morbidity. J Am Soc Nephrol. 1996; 7(4):523–35. [PubMed: 8724885]
2. Gibson KD, et al. Vascular access survival and incidence of revisions: a comparison of prosthetic grafts, simple autogenous fistulas, and venous transposition fistulas from the United States Renal Data System Dialysis Morbidity and Mortality Study. J Vasc Surg. 2001; 34(4):694–700. [PubMed: 11668326]
3. Dixon BS, et al. Effect of dipyridamole plus aspirin on hemodialysis graft patency. N Engl J Med. 2009; 360(21):2191–201. [PubMed: 19458364]
4. Ai D, et al. Angiotensin II up-regulates soluble epoxide hydrolase in vascular endothelium in vitro and in vivo. Proc Natl Acad Sci U S A. 2007; 104(21):9018–23. [PubMed: 17495027]

5. Sanders WG, et al. A biodegradable perivascular wrap for controlled, local and directed drug delivery. J Control Release. 2012; 161(1):81–9. [PubMed: 22561340]
6. Roy-Chaudhury P, et al. Venous neointimal hyperplasia in polytetrafluoroethylene dialysis grafts. Kidney Int. 2001; 59(6):2325–34. [PubMed: 11380837]
7. Shi Y, et al. Adventitial myofibroblasts contribute to neointimal formation in injured porcine coronary arteries. Circulation. 1996; 94(7):1655–64. [PubMed: 8840858]
8. Tsai S, et al. TGF-beta through Smad3 signaling stimulates vascular smooth muscle cell proliferation and neointimal formation. Am J Physiol Heart Circ Physiol. 2009; 297(2):H540–9. [PubMed: 19525370]
9. Roy-Chaudhury P, Sukhatme VP, Cheung AK. Hemodialysis vascular access dysfunction: A cellular and molecular viewpoint. Journal of the American Society of Nephrology. 2006; 17(4): 1112–1127. [PubMed: 16565259]
10. Weiss MF, Scivittaro V, Anderson JM. Oxidative stress and increased expression of growth factors in lesions of failed hemodialysis access. Am J Kidney Dis. 2001; 37(5):970–80. [PubMed: 11325679]
11. Honda HM, et al. A complex flow pattern of low shear stress and flow reversal promotes monocyte binding to endothelial cells. Atherosclerosis. 2001; 158(2):385–90. [PubMed: 11583717]
12. Zeldin DC. Epoxygenase pathways of arachidonic acid metabolism. J Biol Chem. 2001; 276(39): 36059–62. [PubMed: 11451964]
13. Spector AA, Norris AW. Action of epoxyeicosatrienoic acids on cellular function. Am J Physiol Cell Physiol. 2007; 292(3):C996–1012. [PubMed: 16987999]
14. Node K, et al. Anti-inflammatory properties of cytochrome P450 epoxygenase-derived eicosanoids. Science. 1999; 285(5431):1276–9. [PubMed: 10455056]
15. Imig JD. Cardiovascular therapeutic aspects of soluble epoxide hydrolase inhibitors. Cardiovasc Drug Rev. 2006; 24(2):169–88. [PubMed: 16961727]
16. Sun J, et al. Inhibition of vascular smooth muscle cell migration by cytochrome p450 epoxygenase-derived eicosanoids. Circ Res. 2002; 90(9):1020–7. [PubMed: 12016269]
17. Kessler P, et al. Proinflammatory mediators chronically downregulate the formation of the endothelium-derived hyperpolarizing factor in arteries via a nitric oxide/cyclic GMP-dependent mechanism. Circulation. 1999; 99(14):1878–84. [PubMed: 10199886]
18. Node K, et al. Activation of Galpha s mediates induction of tissue-type plasminogen activator gene transcription by epoxyeicosatrienoic acids. J Biol Chem. 2001; 276(19):15983–9. [PubMed: 11279071]
19. Spiecker M, Liao JK. Vascular protective effects of cytochrome p450 epoxygenase-derived eicosanoids. Arch Biochem Biophys. 2005; 433(2):413–20. [PubMed: 15581597]
20. Potente M, et al. Cytochrome P450 2C9-induced endothelial cell proliferation involves induction of mitogen-activated protein (MAP) kinase phosphatase-1, inhibition of the c-Jun N-terminal kinase, and up-regulation of cyclin D1. J Biol Chem. 2002; 277(18):15671–6. [PubMed: 11867622]
21. Skepner JE, et al. Chronic treatment with epoxyeicosatrienoic acids modulates insulin signaling and prevents insulin resistance in hepatocytes. Prostaglandins Other Lipid Mediat. 2011; 94(1-2): 3–8. [PubMed: 21040800]
22. Falck JR, et al. 11,12-epoxyeicosatrienoic acid (11,12-EET): structural determinants for inhibition of TNF-alpha-induced VCAM-1 expression. Bioorg Med Chem Lett. 2003; 13(22):4011–4. [PubMed: 14592496]
23. Krotz F, et al. Membrane-potential-dependent inhibition of platelet adhesion to endothelial cells by epoxyeicosatrienoic acids. Arterioscler Thromb Vasc Biol. 2004; 24(3):595–600. [PubMed: 14715644]
24. Heizer ML, McKinney JS, Ellis EF. 14,15-Epoxyeicosatrienoic acid inhibits platelet aggregation in mouse cerebral arterioles. Stroke. 1991; 22(11):1389–93. [PubMed: 1750047]
25. Pratt PF, Rosolowsky M, Campbell WB. Effects of epoxyeicosatrienoic acids on polymorphonuclear leukocyte function. Life Sci. 2002; 70(21):2521–33. [PubMed: 12173415]
26. Fleming I, Busse R. Endothelium-derived epoxyeicosatrienoic acids and vascular function. Hypertension. 2006; 47(4):629–33. [PubMed: 16490839]

27. Fleming I, et al. The coronary endothelium-derived hyperpolarizing factor (EDHF) stimulates multiple signalling pathways and proliferation in vascular cells. Pflugers Arch. 2001; 442(4):511–8. [PubMed: 11510882]
28. Newman JW, Morisseau C, Hammock BD. Epoxide hydrolases: their roles and interactions with lipid metabolism. Prog Lipid Res. 2005; 44(1):1–51. [PubMed: 15748653]
29. Daikh BE, et al. Regio- and stereoselective epoxidation of arachidonic acid by human cytochromes P450 2C8 and 2C9. J Pharmacol Exp Ther. 1994; 271(3):1427–33. [PubMed: 7996455]
30. Yu Z, et al. Soluble epoxide hydrolase regulates hydrolysis of vasoactive epoxyeicosatrienoic acids. Circ Res. 2000; 87(11):992–8. [PubMed: 11090543]
31. Revermann M, et al. Soluble epoxide hydrolase deficiency attenuates neointima formation in the femoral cuff model of hyperlipidemic mice. Arterioscler Thromb Vasc Biol. 2010; 30(5):909–14. [PubMed: 20224052]
32. Simpkins AN, et al. Soluble epoxide hydrolase inhibition modulates vascular remodeling. Am J Physiol Heart Circ Physiol. 2010; 298(3):H795–806. [PubMed: 20035028]
33. Imig JD, Carpenter MA, Shaw S. The soluble epoxide hydrolase inhibitor AR9281 decreases blood pressuer, ameliorates renal injury and improves vascular function in hypertension. Pharmaceuticals. 2009; 2:217–227.
34. Zhao X, et al. Soluble epoxide hydrolase inhibition protects the kidney from hypertension-induced damage. J Am Soc Nephrol. 2004; 15(5):1244–53. [PubMed: 15100364]
35. Koerner IP, et al. Soluble epoxide hydrolase: regulation by estrogen and role in the inflammatory response to cerebral ischemia. Front Biosci. 2008; 13:2833–41. [PubMed: 17981757]
36. Xu D, et al. Prevention and reversal of cardiac hypertrophy by soluble epoxide hydrolase inhibitors. Proc Natl Acad Sci U S A. 2006; 103(49):18733–8. [PubMed: 17130447]
37. Zhang LN, et al. Inhibition of soluble epoxide hydrolase attenuated atherosclerosis, abdominal aortic aneurysm formation, and dyslipidemia. Arterioscler Thromb Vasc Biol. 2009; 29(9):1265–70. [PubMed: 19667112]
38. Zhang LN, et al. Inhibition of soluble epoxide hydrolase attenuates endothelial dysfunction in animal models of diabetes, obesity and hypertension. Eur J Pharmacol. 2011; 654(1):68–74. [PubMed: 21187082]
39. Schuck RN, et al. Cytochrome P450-derived eicosanoids and vascular dysfunction in coronary artery disease patients. Atherosclerosis. 2013; 227(2):442–8. [PubMed: 23466098]
40. Sanders WG, et al. Soluble epoxide hydrolase expression in a porcine model of arteriovenous graft stenosis and anti-inflammatory effects of a soluble epoxide hydrolase inhibitor. American Journal of Physiology - Cell Physiology. 2012; 303(3):C278–C290. [PubMed: 22621785]
41. Kelly BS, et al. Aggressive venous neointimal hyperplasia in a pig model of arteriovenous graft stenosis. Kidney International. 2002; 62(6):2272–2280. [PubMed: 12427156]
42. Roy-Chaudhury P, et al. Hemodialysis vascular access dysfunction: From pathophysiology to novel therapies. Blood Purification. 2003; 21(1):99–110. [PubMed: 12596755]
43. Roy-Chaudhury P, et al. Cellular phenotypes in human stenotic lesions from haemodialysis vascular access. Nephrol Dial Transplant. 2009; 24(9):2786–91. [PubMed: 19377054]
44. Kuji T, et al. Efficacy of local dipyridamole therapy in a porcine model of arteriovenous graft stenosis. Kidney International. 2006; 69(12):2179–2185. [PubMed: 16672912]
45. Newman JW, et al. Cytochrome p450-dependent lipid metabolism in preovulatory follicles. Endocrinology. 2004; 145(11):5097–105. [PubMed: 15308618]
46. Luria A, et al. Compensatory mechanism for homeostatic blood pressure regulation in Ephx2 gene-disrupted mice. J Biol Chem. 2007; 282(5):2891–8. [PubMed: 17135253]
47. Borhan B, et al. Improved radiolabeled substrates for soluble epoxide hydrolase. Anal Biochem. 1995; 231(1):188–200. [PubMed: 8678300]
48. Yang J, et al. Quantitative profiling method for oxylipin metabolome by liquid chromatography electrospray ionization tandem mass spectrometry. Anal Chem. 2009; 81(19):8085–93. [PubMed: 19715299]
49. Chiamvimonvat N, et al. The soluble epoxide hydrolase as a pharmaceutical target for hypertension. J Cardiovasc Pharmacol. 2007; 50(3):225–37. [PubMed: 17878749]

50. Morisseau C, et al. Structural refinement of inhibitors of urea-based soluble epoxide hydrolases. Biochem Pharmacol. 2002; 63(9):1599–608. [PubMed: 12007563]
51. Li L, et al. PDGF-induced proliferation in human arterial and venous smooth muscle cells: molecular basis for differential effects of PDGF isoforms. J Cell Biochem. 2011; 112(1):289–98. [PubMed: 21069732]
52. Owens GK, Vernon SM, Madsen CS. Molecular regulation of smooth muscle cell differentiation. J Hypertens Suppl. 1996; 14(5):S55–64. [PubMed: 9120686]
53. Thyberg J. Phenotypic modulation of smooth muscle cells during formation of neointimal thickenings following vascular injury. Histol Histopathol. 1998; 13(3):871–91. [PubMed: 9690143]
54. Thyberg J, et al. Phenotypic modulation of smooth muscle cells after arterial injury is associated with changes in the distribution of laminin and fibronectin. J Histochem Cytochem. 1997; 45(6): 837–46. [PubMed: 9199669]
55. Li L, et al. Cellular and morphological changes during neointimal hyperplasia development in a porcine arteriovenous graft model. Nephrol Dial Transplant. 2007; 22(11):3139–46. [PubMed: 17602194]
56. Feng W, et al. EETs and CYP2J2 inhibit TNF-alpha-induced apoptosis in pulmonary artery endothelial cells and TGF-beta1-induced migration in pulmonary artery smooth muscle cells. Int J Mol Med. 2013; 32(3):685–93. [PubMed: 23835530]
57. Davis BB, et al. Inhibitors of soluble epoxide hydrolase attenuate vascular smooth muscle cell proliferation. Proc Natl Acad Sci U S A. 2002; 99(4):2222–7. [PubMed: 11842228]
58. Davis BB, et al. Attenuation of vascular smooth muscle cell proliferation by 1-cyclohexyl-3-dodecyl urea is independent of soluble epoxide hydrolase inhibition. J Pharmacol Exp Ther. 2006; 316(2):815–21. [PubMed: 16221742]
59. Ng VY, et al. Inhibition of smooth muscle proliferation by urea-based alkanoic acids via peroxisome proliferator-activated receptor alpha-dependent repression of cyclin D1. Arterioscler Thromb Vasc Biol. 2006; 26(11):2462–8. [PubMed: 16917105]
60. Itoh T, et al. Structural basis for the activation of PPARgamma by oxidized fatty acids. Nat Struct Mol Biol. 2008; 15(9):924–31. [PubMed: 19172745]
61. Nagy L, et al. Oxidized LDL regulates macrophage gene expression through ligand activation of PPARgamma. Cell. 1998; 93(2):229–40. [PubMed: 9568715]
62. Ozawa T, et al. Biosynthesis of leukotoxin, 9,10-epoxy-12 octadecenoate, by leukocytes in lung lavages of rat after exposure to hyperoxia. Biochem Biophys Res Commun. 1986; 134(3):1071–8. [PubMed: 3947358]
63. Marx N, et al. Peroxisome proliferator-activated receptor gamma activators inhibit gene expression and migration in human vascular smooth muscle cells. Circ Res. 1998; 83(11):1097–103. [PubMed: 9831704]
64. Hsueh WA, Jackson S, Law RE. Control of vascular cell proliferation and migration by PPAR-gamma: a new approach to the macrovascular complications of diabetes. Diabetes Care. 2001; 24(2):392–7. [PubMed: 11213897]
65. Ricote M, et al. The peroxisome proliferator-activated receptor-gamma is a negative regulator of macrophage activation. Nature. 1998; 391(6662):79–82. [PubMed: 9422508]
66. Jiang C, Ting AT, Seed B. PPAR-gamma agonists inhibit production of monocyte inflammatory cytokines. Nature. 1998; 391(6662):82–6. [PubMed: 9422509]
67. Michiels C, et al. Hypoxia stimulates human endothelial cells to release smooth muscle cell mitogens: role of prostaglandins and bFGF. Exp Cell Res. 1994; 213(1):43–54. [PubMed: 8020605]
68. Laniado-Schwartzman M, et al. Activation of nuclear factor kappa B and oncogene expression by 12(R)-hydroxyeicosatrienoic acid, an angiogenic factor in microvessel endothelial cells. J Biol Chem. 1994; 269(39):24321–7. [PubMed: 7523372]
69. O'Flaherty JT, et al. Neutrophil-aggregating activity of monohydroxyeicosatetraenoic acids. Am J Pathol. 1981; 104(1):55–62. [PubMed: 7258296]

70. Natarajan R, et al. Elevated glucose and angiotensin II increase 12-lipoxygenase activity and expression in porcine aortic smooth muscle cells. Proc Natl Acad Sci U S A. 1993; 90(11):4947–51. [PubMed: 8506339]

71. Kawasaki K, et al. Inhibition of 12(S)-hydroxyeicosatetraenoic acid (12-HETE) production suppressed the intimal hyperplasia caused by poor-runoff conditions in the rabbit autologous vein grafts. J Cardiovasc Pharmacol. 2000; 36(5):555–63. [PubMed: 11065214]

72. Al-Shabrawey M, et al. Increased expression and activity of 12-lipoxygenase in oxygen-induced ischemic retinopathy and proliferative diabetic retinopathy: implications in retinal neovascularization. Diabetes. 2011; 60(2):614–24. [PubMed: 21228311]

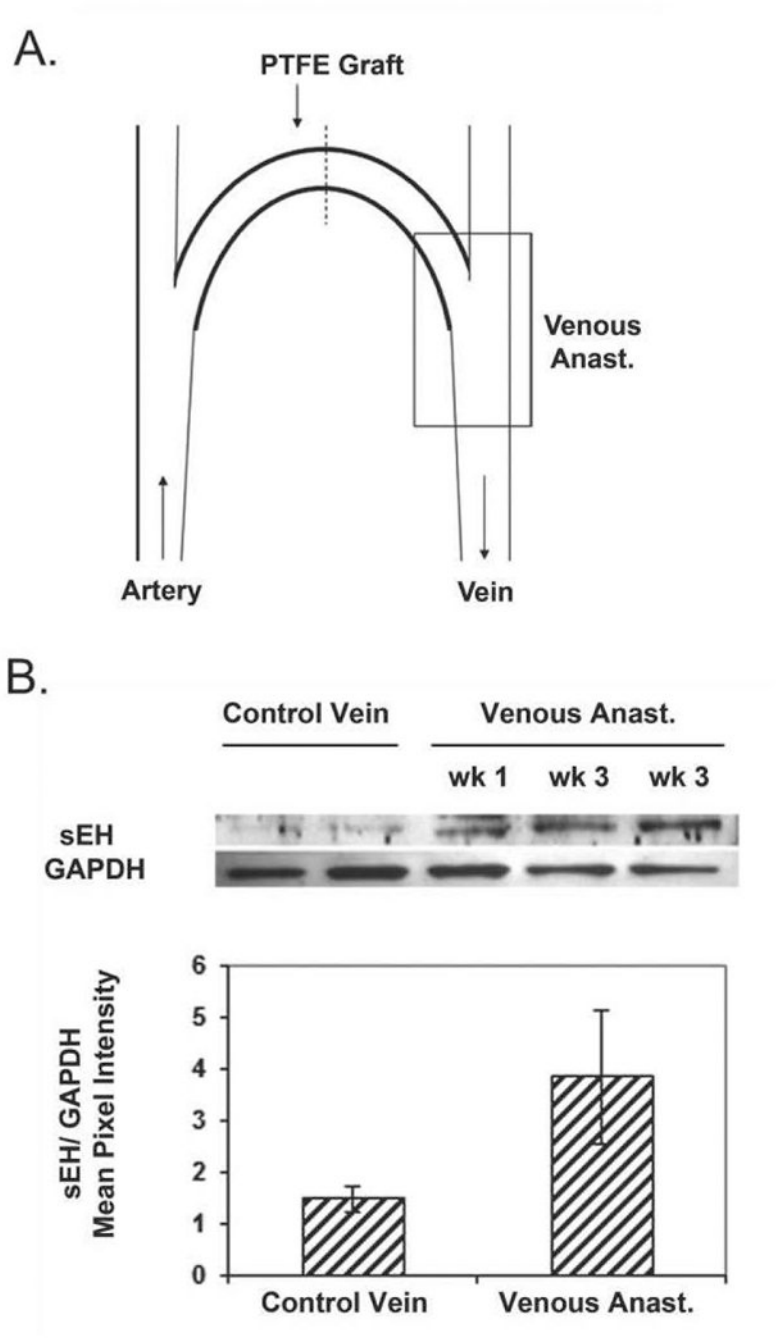

Figure 1.

sEH expression in tissues of the vein-graft anastomosis after AVG placement in the pig. Panel A. Cartoon depicting the PTFE graft placed between the common carotid artery and ipsilateral external jugular vein. The rectangular box outlines the approximate vein-graft anastomotic area that was analyzed for sEH and oxylipins in Figures 1-5. Panel B. Lysates were prepared from the vein-graft anastomotic tissues harvested one week (n=1) or three weeks (n=2) after graft placement or from the normal external jugular vein of an unoperated pig (control vein; n=2) and analyzed by SDS-PAGE followed by immunoblotting with anti-

sEH antibody. Protein loading was assessed by immunostaining with anti-GAPDH antibody. Band intensity from sEH immunostaining was measured and protein loading corrected by dividing by GAPDH band intensity. The normalized sEH band intensity is displayed in a bar graph.

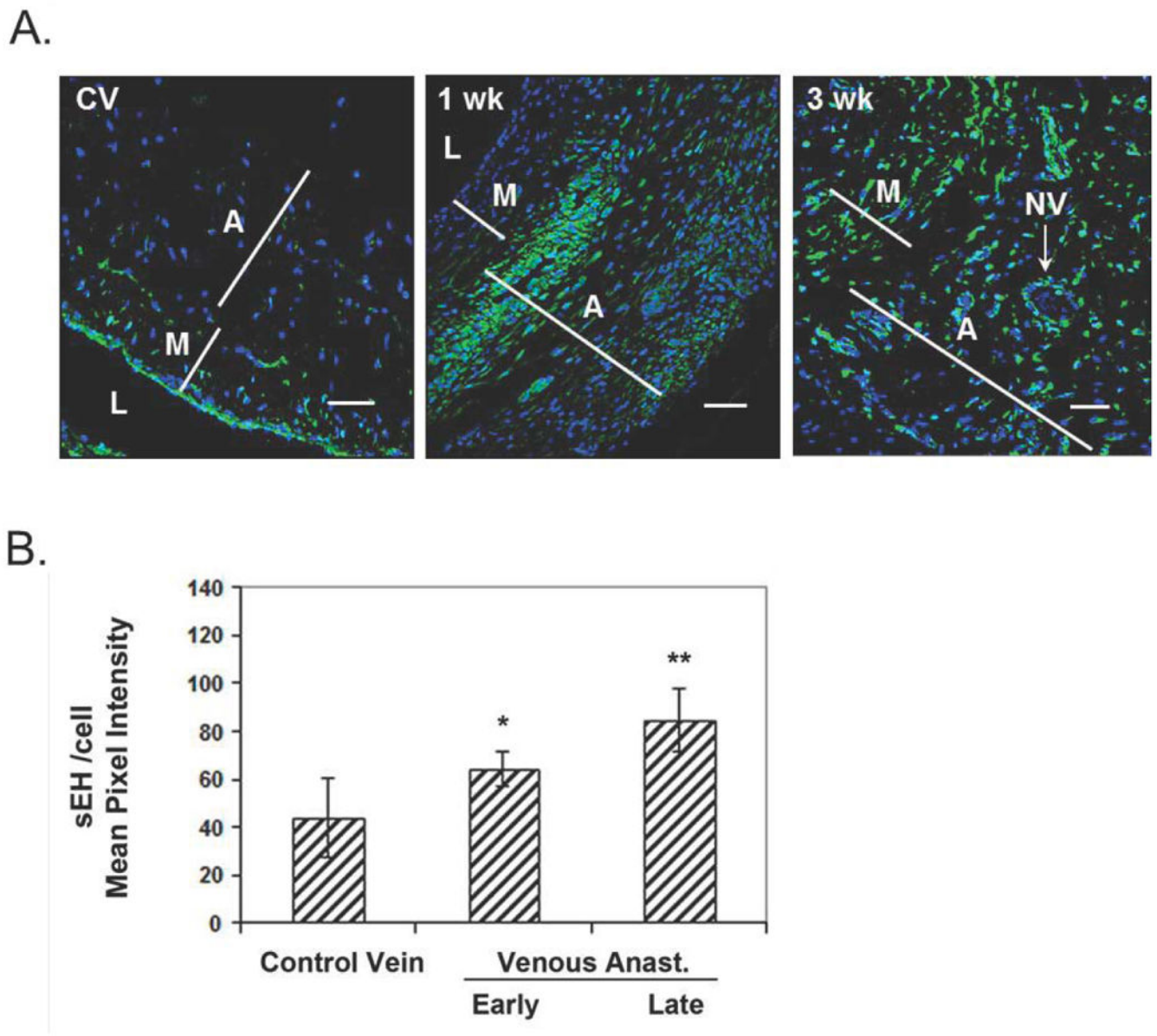

Figure 2.

Expression of sEH in tissues of the vein-graft anastomosis as determined by immunohistofluorescence and confocal laser scanning microscopy. Panel A. Immunohistofluorescent images of anastomotic tissues explanted one or three weeks after AVG placement and images of normal external jugular vein (control vein or CV) at 200x magnification. sEH staining appears green, while the nuclear stain DAPI appears blue. The lumen is designated L, the media M, the adventitia A, and neovessel NV. Scale bars represent 50 μm. Panel B shows composite semiquantitative data of sEH immunostaining intensity in vein-graft tissue collected at early (n=1 at 1 day, n=1 at 3 days and n=3 at 1 week) and later (n=2 at 3 weeks and n=2 at 4 weeks) time points and from control vein (n=4)). After normalization against the cell number, sEH expression at the early time points was significantly higher at the venous anastomosis than that observed in the control vein

(64.3±7.3 pixel density/cell vs. 43.8±16.4 pixel density/cell; *p<0.05). The sEH expression remained elevated at the late time points compared to control vein (84.7±13.0 pixel density/cell vs. 43.8±16.4 pixel density/cell; **p<0.01).

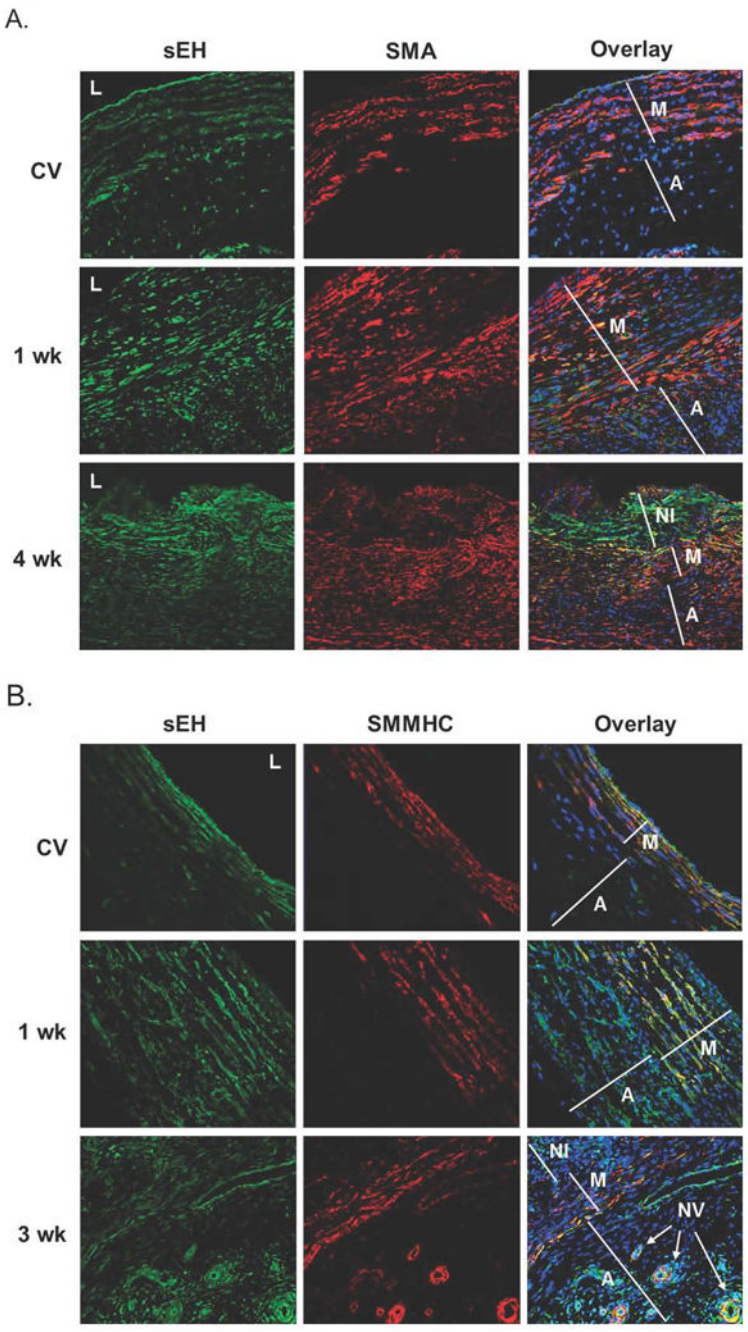

Figure 3.

Characterization of cell types at the vein-graft anastomosis as determined by immunohistofluorescence and confocal laser scanning microscopy. Panel A. Sequential histology sections of the anastomotic tissues, obtained at one week or three weeks, and control veins (CV) were immunostained with anti-sEH (appearing green in left column) or anti-smooth muscle actin α (SMA) (appearing red in middle column) or co-immunostained with anti-sEH, anti-SMA and DAPI (nuclear stain) (sEH = green, SMA = red and DAPI = blue in right column). Co-expression of sEH and SMA appears yellow, or orange if SMA

expression is slightly higher than sEH expression. SMA expression was confined to the medial layer in the control vein with limited co-expression of sEH and SMA. In the anastomotic vein tissue collected at one and four weeks after graft placement, SMA staining was prominent in the adventitia, in addition to the media. Co-staining for sEH and SMA was conspicuous in media at one week and increased in the media and NH at four weeks (overlay panels). Panel B. Sequential histology sections of the anastomotic tissues or control veins were stained with anti-sEH (appearing green in left column), or anti-smooth muscle myosin heavy chain (SMMHC) (appearing red in middle column) or co-immunostained with anti-sEH, anti-SMMHC and DAPI (sEH = green, SMMHC = red and DAPI = blue in right column). In contrast to SMA, staining for SMMHC was not apparent in the adventitia of AVG tissue, except for the three-week time point, when SMMHC could be readily observed in or around the neovascular walls (bottom panel of middle column). Co-staining of SMMHC with sEH (appearing yellow in the overlay in the right column) was evident in the media at one week but largely disappeared at three weeks. In contrast to SMA, co-staining of SMMHC in the neointimal hyperplasia (NH) region was very low at three weeks (overlay in right column). A = Adventitia; L = lumen; M = media; NI = neointima ; NV = neovessel.

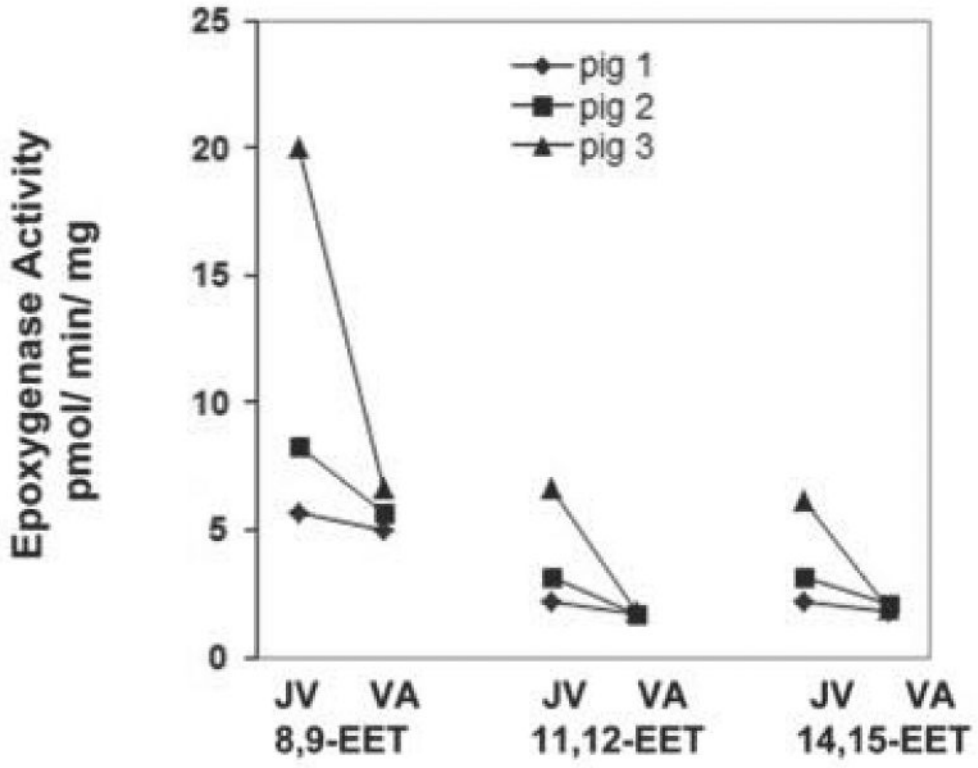

Figure 4.

Epoxygenase and sEH activities in tissues of the vein-graft anastomosis. CYP2C and CYP2J epoxygenase activities were assessed in venous anastomotic (VA) tissues and control veins (CV). The mean levels of 8,9-EET, 11,12-EET and 14,15-EET were lower in the anastomotic tissues than in the control veins ($p<0.001$).

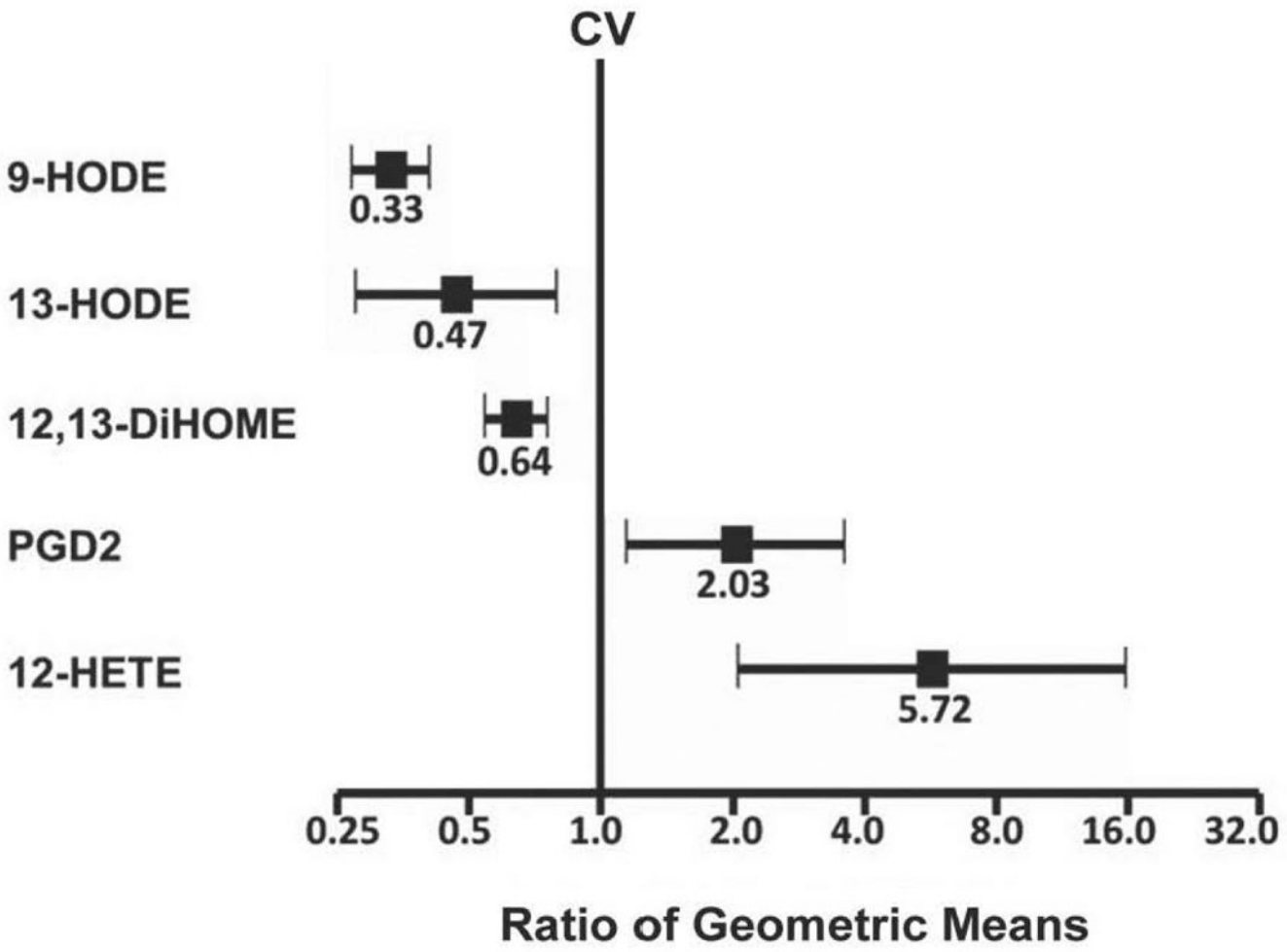

Figure 5.

Five oxylipins whose levels were statistically significantly different between tissues of the vein-graft anastomosis and control venous tissues. The data are displayed as a forest plot of the ratio of geometric means between venous anastomosis (n=3) and control vein (CV; n=3) with 95% confidence intervals. The levels of 9-, and 13-hydroxyoctadecadienoic acid (9-HODE, 13-HODE), and 12,13-dihydroxyoctadecenoic acid (DiHOME) were decreased, while the levels of prostaglandin D_2 (PGD_2) and 12-hydroxyeicosatetraenoic acid (12-HETE) were increased in the anastomotic tissues, compared to control veins ($p<0.05$).

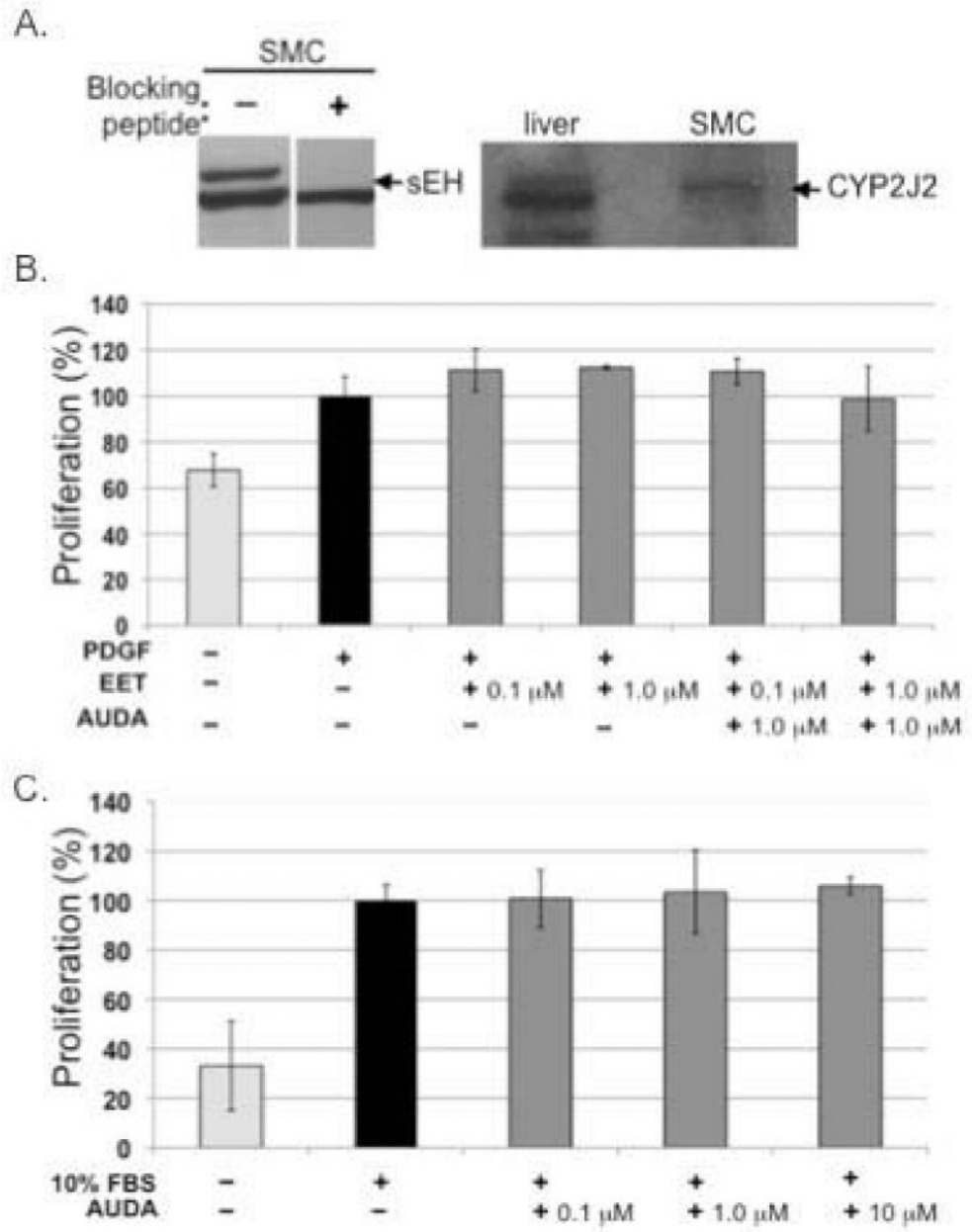

Figure 6.

CYP2J2 and sEH expression in SMC and effect of EETs and/or sEH inhibitor on PDGF-induced proliferation of human SMC or fibroblasts. Panel A. Cell lysates from porcine SMC were size fractionated, transferred then immunostained with anti-sEH antibody in the absence (-) or presence (+) of an sEH-specific blocking peptide (left blot). Lysates from murine liver or human SMC were immunostained with anti-human CYP2J2 antibody which detected a protein of ∼57 kD (right blot). Panel B. SMC were serum-starved and then induced to proliferate with PDGF (50 ng/ml). The addition of EETs (0.1 μM-10 μM) in the absence or presence of the sEH inhibitor AUDA (0.1 μM) did not inhibit proliferation. Panel

B. AUDA (0.1 μM-10 μM) had no significant effect on fibroblast proliferation induced by 10% FBS. Each bar represents the mean ± SD of 3 or 4 observations.

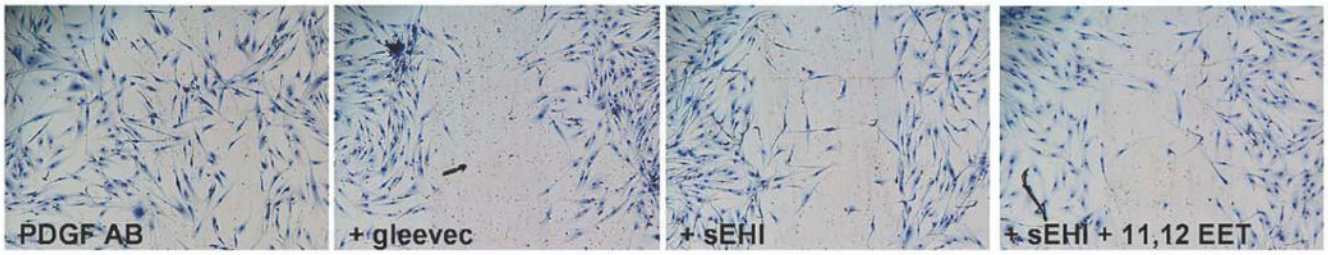

Figure 7.

Effect of sEH inhibitor AUDA (10 μM) and EETs on human SMC migration using a wounding assay. AUDA with or without 11, 12 EET inhibited the inward migration of cells into the wounded area in response to PDGF treatment similar to that seen with a PDGF-receptor inhibitor imatinib.

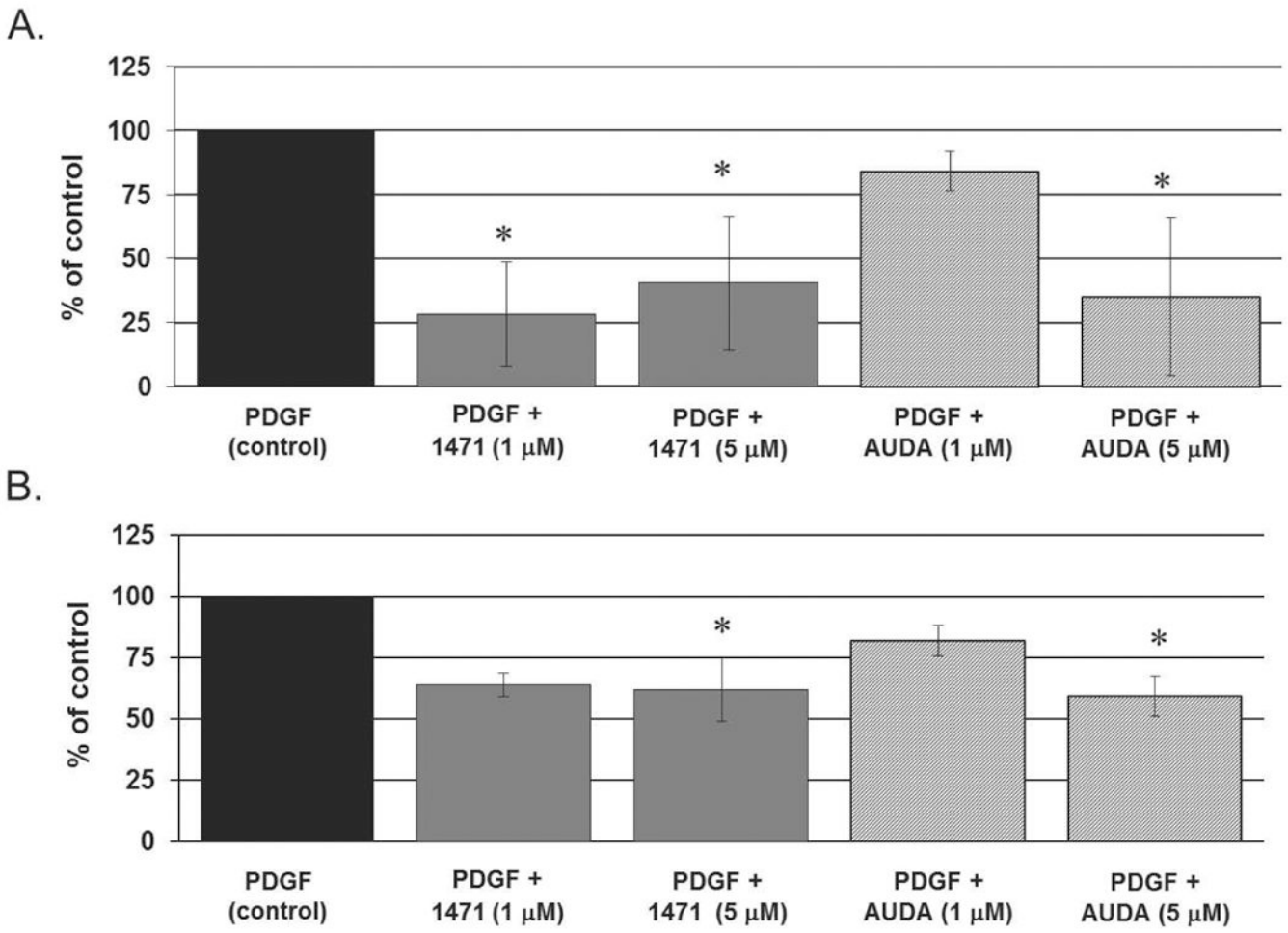

Figure 8.

Effect of sEH inhibitors on PDGF-stimulated migration of human SMC and fibroblasts through a porous membrane. Panel A. Human aortic SMC were seeded in the upper chamber of the migration apparatus after pretreatment with one of two concentrations of either AUDA or *t*-AUCB. Migration is shown as a percent of that seen with PDGF alone without inhibitors. Panel B. Human adventitial fibroblasts were seeded into the upper chamber after pretreatment with one of the two inhibitors. *$p<0.05$ vs. PDGF alone.

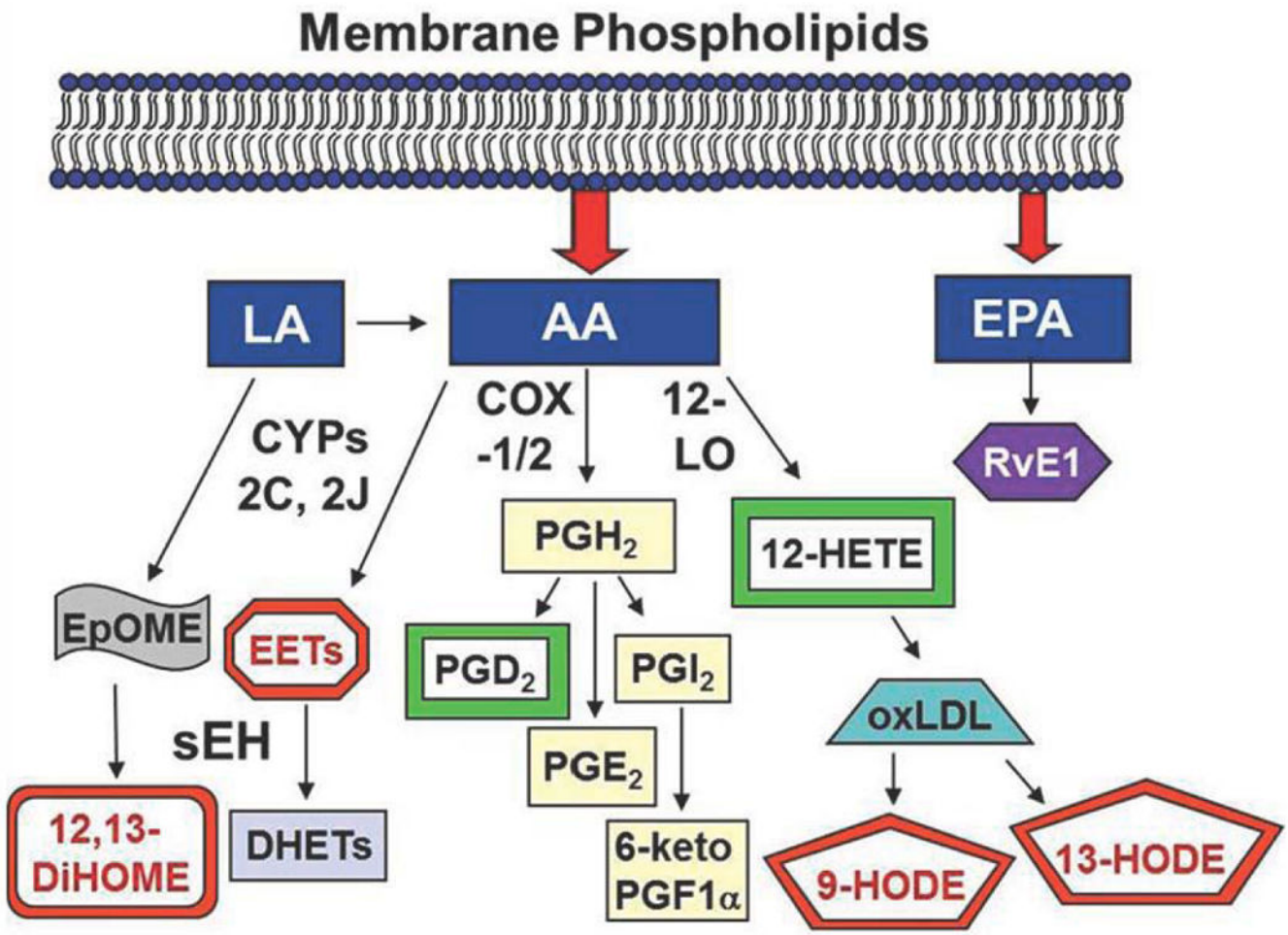

Figure 9.

Proposed cellular arachidonic acid metabolic pathways that contribute to NH formation at vein-graft anastomosis after AVG placement. Moieties that were observed to be decreased in the venous anastomotic tissues, compared to control veins (EETs, 12,13-DiHOME, 9-HODE and 13-HODE), are highlighted by black borders, while moieties that were observed to be increased are highlighted by gray borders. Reduced epoxygenase activity and/or increased sEH activity would contribute to the decreased EET levels and also shunt the polyunsaturated fatty acid substrates to the cyclooxygenase (COX) and lipoxygenase (LO) pathways. The proinflammatory mediators PGD_2 and 12-HETE are produced by COX1/2 and 12-LO enzymes respectively. The observed decreased 9-HODE and 13-HODE levels may be the result of decreased oxidation of LDL. Abbreviation: LA, linoleic acid; AA, arachidonic acid; EPA, eicosapentanoic acid; CYPs 2C, 2J; cytochrome P450 2C or 2J, COX-1/2; cyclooxygenase 1 or 2, 12-LO; 12-lipoxygenase, RvE1, resolvin E1; EpOME; 12,13-epoxyoctadecenoic acid; 12,13-DiHOME, dihydroxyoctadecenoic acid; EETs, epoxyeicosatrienoic acid; sEH, soluble epoxide hydrolase; DHETs, dihydroxyeicosatrienoic acid; PGH_2, prostaglandin H_2; PGD_2, prostaglandin D_2; PGI_2, prostacyclin; PGE_2, prostaglandin E_2; 6-keto $PGF_{1\alpha}$, 6-keto-prostaglandin $F_{1\alpha}$; 12-HETE, 12-

hydroxyeicosatetraenoic acid; oxLDL, oxidized low-density lipoprotein; 9-HODE, 9-hydroxyoctadecadienoic acid; 13-HODE, 13-hydroxyoctadecadienoic acid.

Table 1

Ratio of geometric means of oxylipins in the tissue of the vein-graft anastomoses obtained at 3 weeks after AVG placement to oxylipins in control vein (CV) tissue.

#	Oxylipin	Ratio AVG:CV	95% confidence interval	#	Oxylipin	Ratio AVG:CV	95% confidence interval
1	11-HETE	0.12	0.0-100.6	15	9,10-EpOME	0.79	0.16-3.90
2	6-keto-$PGF_1\alpha$	0.16	0.02-1.45	16	TXB_2	0.81	0.24-2.68
3	PGE_2	0.22	0.01-4.69	17	11,12-DHET	0.87	0.05-15.62
4	Resolvin E_1	0.37	0.07-1.97	18	9,10,13-TriHOME	0.87	0.12-6.35
5	15-deoxy-PGJ_2	0.42	0.04-4.16	19	15-HETE	0.92	0.08-10.80
6	11,12,15-TriHETrE	0.54	0.04-6.74	20	9,12,13-TriHOME	0.97	0.13-7.30
7	LTB_4	0.57	0.09-3.65	21	14,15-DHET	0.97	0.27-3.45
8	9,10-DiHOME	0.57	0.22-1.5	22	5-HETE	1.12	0.63-1.99
9	8,9-DHET	0.58	0.17-1.94	23	11,12-EET	1.21	0.48-3.04
10	15(S)-HETrE	0.59	0.20-1.73	24	14,15-EET	1.22	0.63-2.39
11	9-oxo-ODE	0.68	0.08-5.55	25	15-oxo-ETE	1.33	0.11-15.57
12	LXA_4	0.70	0.28-1.74	26	8,9-EET	1.34	0.18-9.74
13	12,13-EpOME	0.70	0.22-2.27	27	5,6-EET	1.44	0.63-3.31
14	13-oxo-ODE	0.76	0.01-5.86	28	$PGF_{2\alpha}$	1.59	0.35-7.24

6-keto $PGF_1\alpha$, 6-keto-prostaglandin $F_1\alpha$; PGE_2, prostaglandin E_2; $PGF_2\alpha$, prostaglandin $F_2\alpha$; EpOME, epoxyoctadecenoic acid; TXB_2, thromboxane B_2; DHET, dihydroxy eicosatrienoic acid; Resolvin E_1, trihydroxyeicosapentaenoic acid; TriHOME, trihydroxyoctadecenoic acid; 15-deoxy-PGJ_2, 15-deoxy-prostaglandin J_2; HETE, hydroxyeicosatetraenoic acid; TriHETrE, trihydroxyeicosatrienoic acid; LTB_4, leukotriene B_4; DiHOME, dihydroxyoctadecenoic acid; EET, epoxyeicosatrienoic acid; 15(S)-HETrE, hydroxyeicosatrienoic acid; 15-oxo-ETE, oxo-eicosatetraenoic acid; 9-oxo-ODE, oxooctadecadienoic acid; LXA_4, lipoxin A_4.